Neurobiology of Aging 116 (2022) 80–91

Contents lists available at ScienceDirect

Neurobiology of Aging

journal homepage: www.elsevier.com/locate/neuaging.org

Relationship between cerebrospinal fluid neurodegeneration biomarkers and temporal brain atrophy in cognitively healthy older adults

Didac Vidal-Piñeiro[a,*], Øystein Sørensen[a], Kaj Blennow[b,c], Elettra Capogna[a], Nathalie Bodd Halaas[d,e], Ane-Victoria Idland[d,e], Athanasia Monica Mowinckel[a], Joana Braga Pereira[f,g], Leiv Otto Watne[d], Henrik Zetterberg[b,c,h,i,j], Kristine Beate Walhovd[a,k], Anders Martin Fjell[a,k], the Alzheimer's Disease Neuroimaging Initiative[#]

[a] Center for Lifespan Changes in Brain and Cognition, Department of Psychology, University of Oslo, Oslo, Norway
[b] Institute of Neuroscience and Physiology, the Sahlgrenska Academy at University of Gothenburg, Mölndal, Sweden
[c] Clinical Neurochemistry Laboratory, Sahlgrenska University Hospital, Mölndal, Sweden
[d] Oslo Delirium Research Group, Department of Geriatric Medicine, Oslo University Hospital, Oslo, Norway
[e] Institute of Clinical Medicine, University of Oslo, Oslo, Norway
[f] Clinical Memory Research Unit, Department of Clinical Sciences, Lund University, Malmo, Sweden
[g] Division of Clinical Geriatrics, Department of Neurobiology, Care Sciences and Society, Karolinska Institute, Stockholm, Sweden
[h] Department of Neurodegenerative Disease, UCL Institute of Neurology, London, UK
[i] UK Dementia Research Institute at UCL, London, UK
[j] Hong Center for Neurodegenerative Diseases, Hong Kong, China
[k] Department of radiology and nuclear medicine, Oslo University Hospital, Oslo, Norway

ARTICLE INFO

Article history:
Received 1 October 2021
Revised 5 April 2022
Accepted 14 April 2022
Available online 22 April 2022

Keywords:
Cognitively healthy older adults
Neurodegeneration biomarkers
FABP3
Neurogranin
NFL
CSF

ABSTRACT

It is unclear whether cerebrospinal fluid (CSF) biomarkers of neurodegeneration predict brain atrophy in cognitively healthy older adults, whether these associations can be explained by phosphorylated tau181 (p-tau) and the 42 amino acid form of amyloid-β (Aβ42) biomarkers, and which neural substrates may drive these associations. We addressed these questions in 2 samples of cognitively healthy older adults who underwent longitudinal structural MRI up to 7 years and had baseline CSF levels of heart-type fatty-acid binding protein (FABP3)=, total-tau, neurogranin, and neurofilament light (NFL) (n = 189, scans = 721). The results showed that NFL, total-tau, and FABP3 predicted entorhinal thinning and hippocampal atrophy. Brain atrophy was not moderated by Aβ42 and the associations between NFL and FABP3 with brain atrophy were independent of p-tau. The spatial pattern of cortical atrophy associated with the biomarkers overlapped with neurogenetic profiles associated with expression in the axonal (total-tau, NFL) and dendritic (neurogranin) components. CSF biomarkers of neurodegeneration are useful for predicting specific features of brain atrophy in older adults, independently of amyloid and tau pathology biomarkers.

1. Introduction

Longitudinal structural magnetic resonance imaging (MRI) measures such as hippocampal (HC) shrinkage and entorhinal cortex (EC) thinning are seen both in cognitively healthy older adults (OA) and in Alzheimer's Disease (AD). In OA, these MRI metrics are related to intraindividual variability in cognition, especially in memory (Gorbach et al., 2017). In AD, these indices are widely used as biomarkers of neurodegeneration providing nonspecific information about neuronal injury and neurodegenerative change,

* Corresponding author at: Center for Lifespan Changes in Brain and Cognition, Department of Psychology, University of Oslo, Oslo, Norway, Tel.: +47-22845061.
E-mail address: d.v.pineiro@psykologi.uio.no (D. Vidal-Piñeiro).

[#] Data used in preparation of this article were partially obtained from the Alzheimer's Disease Neuroimaging Initiative (ADNI) database (adni.loni.usc.edu). As such, the investigators within the ADNI contributed to the design and implementation of ADNI and/or provided data but did not participate in the analysis or writing of this report. A complete listing of ADNI investigators can be found at http://adni.loni.usc.edu/wpcontent/uploads/how_to_apply/ADNI_Acknowledgement_List.pdf.

0197-4580/$ – see front matter © 2022 The Author(s). Published by Elsevier Inc. This is an open access article under the CC BY license (http://creativecommons.org/licenses/by/4.0/)
https://doi.org/10.1016/j.neurobiolaging.2022.04.010

aligning closely to cognitive decline and dementia, and forming part of diagnostic guidelines and consensus AD criteria (Hill et al., 2014; Jack et al., 2018). However, cross-sectional MRI measures have limited validity as indices of brain atrophy particularly in OA (Joie et al., 2020; Vidal-Pineiro et al., 2021) since lifelong differences - that is *intercept* differences – and not ongoing neurodegeneration - *slope* changes - are the main source of interindividual variability in brain structure (Tucker-Drob, 2019). Presently, we have access to multiple CSF biomarkers that are thought to reflect ongoing neurodegeneration. It is thus important to determine how different CSF biomarkers of neurodegeneration in OA are related to brain atrophy as measured by serial MRI if the relationship between these biomarkers and atrophy are moderated by the core AD biomarkers of Amyloid-βeta (Aβ) and phosphorylated tau181 (p-tau), and which cellular and molecular substrates might drive biomarker-related changes in cortical thinning. Thus, we aimed to, first, assess the relationship between 4 different cerebrospinal fluid (CSF) (FABP3, t-tau, neurogranin, and NFL) markers – at baseline - capturing different aspects of neurodegeneration and prospective hippocampus (HC) atrophy and entorhinal cortex (EC) thinning - up to 7 years. Second, assess whether these biomarker-brain relationships are moderated by core AD biomarkers p-tau and Aβ and the presence of the apolipoprotein ε4 (APOE ε4) allele. Third, inform on tentative neural substrates underlying biomarker-related changes in cortical thinning through the use of neurogenetic analyses (Groot et al., 2021).

Different aspects of neurodegeneration that appear with advancing age and with the development of AD can be measured via CSF markers (DeKosky and Golde, 2016; Obrocki et al., 2020; Pereira et al., 2021; Wyss-Coray, 2016). Heart-type fatty acid-binding protein 3 (FABP3 [also known as HFABP]) is a protein involved in the metabolism and transport of fatty acids (Moullé et al., 2012) and is expressed in the brain neurons (Pelsers et al., 2004). CSF FABP3 is considered a biomarker of neuronal damage as it is released following cellular injury, possibly reflecting lipid dyshomeostasis (Desikan et al., 2013; Dhiman et al., 2019). Neurofilament light chain protein (NFL) is a protein of the neural cytoskeleton involved in axonal and dendritic homeostasis and synaptic transmission (Khalil et al., 2018; Lépinoux-Chambaud and Eyer, 2013; Petzold, 2005). CSF NFL is considered a marker of neuroaxonal damage (Bridel et al., 2019). Neurogranin (Ng) is a calmodulin-binding post-synaptic protein, expressed in dendritic spines and memory processing regions, involved in long-term potentiation and memory consolidation (Díez-Guerra, 2010; Pak et al., 2000). CSF total tau (t-tau) is generally considered a marker of neuronal damage, released with cell death and injury, though in OA is often closely associated with the levels of hyperphosphorylated Tau (p-tau) which is regarded as a more specific AD biomarker (Hampel et al., 2010; Zetterberg and Blennow, 2018).

In OA, it is still unclear whether these CSF biomarkers mostly capture neurodegenerative changes associated with early AD pathology or reflect manifold biological events co-occurring in the aging brain (Boyle et al., 2021, 2018). On one side, levels of these CSF biomarkers are increased throughout different AD stages, predicting clinical progression and severity, and being associated with cross-sectional brain features as well as brain atrophy (Desikan et al., 2013; Dhiman et al., 2019; Gangishetti et al., 2018; Iturria-Medina et al., 2016; Pereira et al., 2021; Portelius et al., 2015). However, in OA, some of these CSF biomarkers may be unspecific to AD, as they increase with age independently of amyloid deposition (Idland et al., 2020) and are also present in other age-related pathologies (Chiasserini et al., 2017; Gattringer et al., 2017). Although these CSF biomarkers are moderately to highly correlated in OA (Idland et al., 2020), they yield information about different mechanisms and processes. This knowledge can be used to better understand the biological basis of structural MRI changes in OA, the leading hypothesis being that it mostly reflects neuropil loss (Márquez and Yassa, 2019).

Here we addressed the following questions: First, we tested whether CSF biomarkers of neurodegeneration predict longitudinal atrophy in brain structures with high vulnerability to neurodegeneration (i.e., hippocampal [HC] volume loss and thinning of the entorhinal cortex [EC]). We addressed this question using a 2-fold approach: employing traditional linear mixed model analyses and using Generalized Additive Mixed Models (GAMM) to study possible non-linear relationships between the CSF and longitudinal MRI indices. Second, we studied to which degree the relationships between CSF biomarkers and brain atrophy were explained or moderated by the core AD biomarkers the 42 amino acid form of amyloid-β (Aβ42) and p-tau as well as by carrying the APOE ε4 allele. We studied whether Aβ42 status and carrying an APOE ε4 allele moderated the relationship between CSF biomarkers and brain atrophy and whether the relationships could be explained by introducing p-tau in the models. We also used machine learning to identify the markers that most closely explained brain atrophy. Third, we tested whether the CSF biomarkers reflect different cellular aspects of brain atrophy to inform on normal-aging processes associated with cortical atrophy. We compared the spatial patterns of cortical atrophy associated with each biomarker with the spatial patterns of gene expression associated with specific cellular components.

2. Methods

2.1. Participants

A total of 189 cognitively healthy older individuals (mean age = 74.8 [SD = 5.2] years) were included in the study. Individuals belonged to 2 different cohorts: The *COGNORM* Cohort (Idland et al., 2017) (n = 85) and the *Alzheimer's Disease Neuroimaging Initiative* (ADNI) (Mueller et al., 2005) (n = 104). Both studies were conducted in accordance with the Declaration of Helsinki and approved by the appropriate ethical committees. All participants included in the present study provided written consent. To be included, participants were required to be $\geq$ 65 years old, cognitively healthy based on multiple neuropsychological criteria (e.g., memory scales, Mini Mental State Examination [MMSE] [Folstein et al., 1975], Clinical Dementia Rating [CDR] scale [Morris, 1993]), and have available baseline CSF data at baseline as well as MRI and cognitive follow-ups. Participants that converted to mild cognitive impairment (MCI) or AD during the MRI follow-up were excluded from the analysis, thus retaining only asymptomatic individuals at the time of the last follow-up. See the main sociodemographic and cohort characteristics in Table 1. ADNI participants were, on average, slightly older ($\simeq$ 2.2 years), had more education ($\simeq$ 1.6 years), had fewer APOE ε4 carriers, and lower percentage of amyloid-positive individuals. See specific definitions of cognitively healthy participants, recruitment details, and inclusion criteria in each cohort in Supplementary Methods. Change in cognition over time was within the expected range. Episodic memory was stable over time; global cognitive function showed a very modest decline, while executive function worsened over time in both cohorts. Note that test-retest effects likely affect the longitudinal trajectories of cognition. The cognitive trajectories are described in Supplementary Results and Fig. S1.

2.2. MRI acquisition and preprocessing

T1-weighted (T1w) magnetization prepared rapid gradient echo (MPRAGE) sequences were obtained for all participants. In COG-

Table 1
Data overview grouped by cohort.

	COGNORMN/$\bar{M}$ (SD)	ADNIN/$\bar{M}$ (SD)	ALLN/$\bar{M}$(SD)	Cohort diff.χ^2[p]) / (t[p])
Participants (n)	85	104	189	–
MRI obs. (n)	250	471	721	–
Age	73.6 (6.8)	75.8 (5.2)	74.8 (5.2)	2.41 (.02)
Sex (M:F)	42:43	50:53	96:93	0.00 (1.00)
Education (yrs)	14.1 (3.4)	15.7 (2.9)	15.0 (3.2)	3.3 (.001)
MRI follow-up	4.3 (2.2)	2.9 (1.5)	3.5 (1.9)	-5.1 (<.001)
MMSE	29.1(1.1)	29.1(1.0)	29.1(1.1)	0.51 (.61)
APOE ε4[a]	48:30	82:21	119:45	6.50 (.01)
Aβ42 status (±)[b]	29:56	15:88	44:144	10.00 (.002)

APOE ε4 (non-carrier:carrier). Aβ42 status (Aβ+:Aβ-). Cohort differences are assessed using chi-squared tests (χ^2[p]) for dichotomous variables and t-tests (t[p]) for continuous.
Key: Obs., observations; diff. = differences; MMSE, Mini Mental State Examination.
[a] 4 participants had missing APOE ε4 data in the COGNORM and 1 in the ADNI cohort.
[b] 1 participant with missing data in the ADNI cohort. Sex (Male:Female).

NORM, T1w sequences were acquired with a 1.5T Siemens Avanto (Siemens Medical Solution) with the following parameters: TR/TE/TI = 2400 ms/3.79 ms/1000 ms, FOV = 240, sagittal slices with voxel size = 1.25 × 1.25 × 1.2 mm, 12-channel head coil. ADNI participants included in the analyses were scanned using 1.5T scanners. The T1w MPRAGE parameters slightly varied due to differences in scanners and vendors. MRI image selection was based on the *ADNIMERGE.csv* file. See more information at http://adni.loni.usc.edu/methods/mri-tool/mri-analysis.

Data were processed on the Colossus processing cluster, University of Oslo. We used the longitudinal FreeSurfer v.6.0. stream (Reuter et al., 2012) for cortical reconstruction of the structural T1w data (http://surfer.nmr.mgh.harvard.edu/fswiki) (Dale et al., 1999; Fischl et al., 1999). See preprocessing details in Supplementary Methods. We selected HC (volume) and EC (thickness) as regions of interest (ROI) (averaged across hemispheres) for further analysis as they are highly vulnerable to both AD and aging. For comparison with gene expression data, we extracted thickness data from the n = 34 bilateral cortical ROIs of the Desikan-Kiliany atlas (Desikan et al., 2006), averaged across hemispheres.

2.3. CSF collection and analysis

COGNORM: CSF acquisition details are described elsewhere (Idland et al., 2020, 2017). Briefly, samples were analyzed in the Clinical Neurochemistry Laboratory at Sahlgrenska University Hospital, Mölndal, Sweden. CSF Aβ42, t-tau, and p-tau concentrations were measured using INNOTEST enzyme-linked immunosorbent assay (ELISA; Fujirebio, Ghent, Belgium), CSF NFL concentrations using a commercial ELISA (Uman Diagnostics, Sweden), CSF FABP3 concentrations using an immunoassay with electrochemiluminescence detection (MSD Human FABP3 kit; Meso Scale Discovery, Gaithersburg, MD) and CSF Ng concentrations using an in-house ELISA, as previously described (Portelius et al., 2015). Intra assay coefficients of variation were 9%–13%. ADNI: CSF acquisition details are described elsewhere (Shaw et al., 2011, 2009) (see also http://www.adni-info.org). Briefly, samples were analyzed by the ADNI Biomarker Core laboratory at the University of Pennsylvania Medical Center on dry ice. CSF Aβ42, t-tau, and p-tau biomarkers were measured using Elecsys total-tau, phosphorylated-tau 181 (p-tau), and β-amyloid (1–42) CSF immunoassays (Bittner et al., 2016; Hansson et al., 2018) (*UPENNBIOMK9.csv* ADNI file). Values above the upper technical limit were recalculated based on the calibration curve (≥1700 pg/ml for Aβ42 [n = 19]). CSF FABP3 was quantified with a multiplex-based immunoassay panel, based on Luminex xMAP immunoassay technology and developed by Rules Based Medicine (MyriadMBM) (Olsson et al., 2013) (*CSF_QC_Multiplex_Data.csv* ADNI file). Ng (*BlennowCSFNG.csv* ADNI file) and NFL (*BlennowCSFNFL.csv* ADNI file) were quantified at the Clinical Neurochemistry Laboratory, University of Gothenburg, Sweden, with commercial ELISA for NFL (NF-light ELISA, UmanDiagnostics, Sweden) (Zetterberg et al., 2016) and a CSF Ng in-house ELISA. Missing data was n = 1 for Aβ, p-tau, t-tau, and NFL; n = 3 for NG; and n = 20 for FABP3. See CSF values grouped by cohort in Table S1.

2.4. Statistical Analysis

CSF values were Z-standardized within each cohort to remove possible differences in CSF concentration quantification. We visually inspected the density plots to ensure CSF values were – to a certain extent – normally distributed. Aβ status was obtained by dichotomizing Aβ into Aβ^+ < 550 pg/mL ≥ and Aβ^- groups in both cohorts. Female, COGNORM, and Aβ^- were established as the reference levels. All analyses were run in the R-environment (R Development Core Team, 2012) (https://www.r-project.org). All linear mixed models included Sex, Baseline age, and Cohort as covariates and participant identifiers as random intercepts (estimated intracranial volume [eICV] was also included as a covariate for HC). Note that our study had a descriptive character. For this reason, we did not address the issue of multiple comparisons across biomarkers (n = 4) or brain regions (n = 2). Rather, we corrected for multiple comparisons when multiple tests were carried out to answer the same question (e.g., Biomarker × Aβ interactions using different thresholds for defining Aβ positivity).

2.4.1. Correlations between CSF biomarkers and MRI features at baseline

We computed the (unadjusted) Spearman's ρ cross-correlation matrices between age, the AD core biomarkers (p-tau, Aβ), the neurodegeneration CSF biomarkers, and brain volume and/or thickness at baseline. We used the participant's random intercept as the EC thickness and HC volume estimates based on linear mixed models that also included Cohort as fixed effects. Further, the same Spearman's ρ cross-correlation matrix between MRI and CSF markers was obtained after adjusting for Age and Sex. Both the adjusted and unadjusted matrices were also obtained separately for each cohort. The similarity between the matrices was assessed using a Mantel test and 10.000 permutations.

2.4.2. Effects of CSF neurodegeneration markers on brain features at baseline and brain atrophy

We assessed the associations between the CSF neurodegeneration biomarkers with EC thickness and HC volume using linear mixed-effects models as implemented in the *nlme* R-package. The linear mixed-effects models fitted EC thickness and HC

volume on Biomarker (t-tau, NFL, Ng, FABP3), Time, and the Time × Biomarker interaction. For interpretation purposes, we report Time × Biomarker effects as % of change of ± 1SD in the biomarker compared to mean decline and Biomarker effects as % of the difference of ±1SD in the biomarker compared to mean thickness/volume. Finally, the same models were run using a generalized additive mixed models (GAMM) framework as implemented in the gamm4 R-package (https://cran.r-project.org>package=gamm4) which is capable of fitting nonlinear relationships through local smoothing effects (Sørensen et al., 2021). We used 5 knots and thin plate smoothing splines to fit the smoothed effects of Time, Biomarker, and Time × Biomarker interaction. To assess non-linear trends on the Time × Biomarker contrast, we focused on the estimated degrees of freedom (edf) of the interaction term which informs about the degree of complexity of a curve.

2.4.3. Impact of Aβ and p-tau, and APOE ε4 on the relationship between CSF markers of neurodegeneration and brain atrophy

We performed 3 different analyses to understand the role of AD pathology on the relationship between the CSF biomarkers and brain atrophy. First, we assessed whether Aβ status interacted with the neurodegeneration CSF biomarkers in predicting brain volume and/or thickness at baseline and brain atrophy. We used similar models as above, additionally including Aβ status in the model as well as its interaction with Time and the neurodegeneration CSF biomarkers. As post-hoc analyses, we re-ran the analyses using different thresholds to define Aβ positivity (12 thresholds, based on sample quantiles [0.05,0.5, 0.025]). We used a resampling-based approach that accounted for the dependency of the data as the different tests with varying Aβ positivity thresholds are not independent. In brief, a null distribution (n = 5000) was obtained by selecting, for each permutation, the lowest *p*-value amongst n = 12 identical analyses run with a different Aβ status definition. Second, we introduced APOE ε4 in the previous models. Third, we assessed whether p-tau accounted for the relationships between the CSF biomarkers and brain atrophy. We used similar models as above additionally including p-tau and p-tau × Time in the model. Note that we did not include a triple order interaction in the model (i.e., Biomarker × p-tau × Time). Forth, we used a LASSO algorithm (Tibshirani, 1996) as implemented in the *glmnet* R-package to select the CSF biomarkers that best predicted hippocampal and entorhinal decline. LASSO is a regression-based machine learning analysis that performs variable selection (and regularization) to maximize prediction accuracy (see Supplementary Methods for details).

2.4.5. Effects of CSF neurodegeneration markers on whole-brain volumes

As suggested by a reviewer, we performed all the above-mentioned linear mixed-effect analyses using whole-brain measures. Specifically, we used cortex volume and supratentorial volume, that is, white, and grey matter volume after excluding the brain stem and the cerebellum. See results in Supplementary Results and Table S2.

2.4.6. Spatial association between cellular-component specific gene expression and the cortical thinning maps associated with CSF biomarkers

We compared the spatial maps of cortical decline associated with each CSF biomarker of neurodegeneration and the spatial patterns of gene expression associated with specific cellular components. To obtain the cortical signatures associated with CSF biomarkers, we applied the main model described above to n = 34 bilateral cortical ROIs. For each region, the Time × CSF estimate was considered as the index of interest. For completeness, the full-brain models were rerun using Aβ status and p-tau as described above (Fig. S2). The spatial similarity between the CSF-related cortical thinning maps was assessed using a Spearman's ρ cross-correlation matrix.

See full description of gene expression preprocessing and analyses in Supplementary Methods. Briefly, gene expression maps were computed based on microarray expression data provided by the Allen Human Brain Atlas (https://human.brain-map.org) (Hawrylycz et al., 2012). Data were processed with the *abagen* toolbox (https://github.com/rmarkello/abagen) (Markello et al., 2021). The aggregate metric was set to the *median* while samples were mirrored *bidirectionally* across hemispheres (Romero-Garcia et al., 2018). The remaining parameters were left to default. Data from bilateral ROIs were combined yielding a regional expression matrix with 34 brain regions and 15.633 retained genes. Note, that the analysis was restricted to the cerebral cortex due to the relative heterogeneity compared to subcortical structures (Hawrylycz et al., 2012). Next, we assessed the correlation between the spatial maps associated with CSF-related cortical thinning and gene expression for specific cellular components based on the gene ontology from MsigDB (http://www.gsea-msigdb.org/gsea/index.jsp) (Subramanian et al., 2005) yielding n = 467 gene sets reflecting different aspects of cellular anatomy. We computed the Pearsons's spatial correlation between the CSF-related cortical thinning maps and each gene and combined the mean scores of genes annotated to each category. Statistical significance was assessed using a permutation test that compared the empirical correlation of each gene set to a null distribution that maintained the spatial relationship of the empirical phenotype (cortical thinning maps) (n = 40.000) (*BrainSMASH* package) (Burt et al., 2020). In essence, we tested for spatial specificity; that is, are genes expressed in a specific cellular component more correlated to the CSF-related cortical thinning maps than to random spatially autocorrelated phenotypes? The top 5-hits were reported, together with either a False discovery rate (FDR) correction for multiple comparisons or the uncorrected p-values.

Table 2
Cross-Correlation Biomarker matrix.

	Age	Aβ	p-tau	t-tau	NFL	NG	FABP3	EC	HC
Age	–	–	–	–	–	–	–	–	–
Aβ	-.04	–	.10	.12	.05	.16	.10	.06	.09
p-tau	.20	.10	–	.97	.34	.82	.69	.00	.03
t-tau	.23	.12	.97	–	.36	.83	.69	.00	.04
NFL	.40	.03	.41	.44	–	.26	.36	-.10	-.11
NG	.14	.15	.83	.85	.32	–	.60	-.07	.01
FABP3	.25	.10	.69	.69	.43	.61	–	-.10	-.03
EC	-.38	.04	-.06	-.08	-.24	-.09	-.17	–	.16
HC	-.54	.07	-.09	-.09	-.29	-.06	-.14	.36	–

All samples included (n = 189). Spearman's ρ correlation between Baseline age, CSF, and MRI biomarkers. The lower and upper triangular matrix shows unadjusted and Sex, Age-adjusted correlations, respectively. HC volume was additionally corrected for estimated intracranial volume (eICV). $p < 0.05$ correlations are highlighted.
Key: NFL, Neurofilament light; NG, Neurogranin; FABP3, Heart-type fatty acid-binding protein 3; EC, Entorhinal cortex thickness; HC, Hippocampal volume.

3. Results

3.1. CSF biomarkers correlations

Table 2 shows the ranked cross-correlation between the CSF markers of neurodegeneration, age, and baseline estimates of EC thickness and HC volume both unadjusted and adjusted by age and sex. The 4 CSF markers of neurodegeneration were correlated with each other (Spearman's ρ ranging from .26 to .85) and with

Table 3
Effects of neurodegeneration CSF biomarkers on brain atrophy (Time × Biomarker interaction) and brain at baseline (Biomarker effect).

MRI	Biomarker	Biomarker		Time × Biomarker	
		β(SE)	t(df,p)	β(SE)	t(df,p)
EC	t-tau	-0.14(.54)	-0.26(183,.79)	-19.81(8.62)	-2.30(526,.02)
	NFL	-0.41(.60)	-0.69(183,.49)	-31.84(8.32)	-3.83(526,<.001)
	NG	-0.63(.55)	-1.14(181,.26)	-11.52(8.83)	-1.30(521,.19)
	FABP3	-0.66(.60)	-1.10(164,.27)	-23.58(8.65)	-2.72(477,.006)
HC	t-tau	0.23(.68)	0.33(183,.74)	-14.38(3.60)	-4.00(525, <.001)
	NFL	-0.27(.75)	-0.36(183,.72)	-13.13(3.50)	-3.75(525,<.001)
	NG	-0.09(.70)	-0.13(181,.90)	-5.16(3.65)	-1.41(524,.15)
	FABP3	-0.12(.74)	-0.17(164,.87)	-8.04(3.79)	-2.12(476,.03)

β-estimates for the Time × Biomarker effects reflect the % of change of ±1SD in the Biomarker compared to mean decline. β-estimates for the Biomarker effects reflect the % of difference of ±1SD in the biomarker compared to mean thickness/volume.
Key: df, degrees of freedom; SE, standard error; NFL, Neurofilament light; NG, Neurogranin; FABP3, Heart-type fatty acid-binding protein 3; EC, Entorhinal Cortical Thickness; HC, Hippocampal volume. See Fig. 1 for a visual representation.

p-tau but not Aβ (except Ng [ρ = .15/.16 unadjusted and/or age, sex-adjusted]). When adjusted for Age and Sex, HC volume and EC thickness at baseline were not significantly related neither to the CSF markers of neurodegeneration nor to the AD core biomarkers. The cross-correlation biomarker matrices for the *ADNI* and the *COGNORM* cohorts were comparable as assessed by Mantel tests (r = 0.64, p = 0.005/r = 0.66, p = 0.002 for unadjusted and/or sex, age-adjusted ranked distances). Both were comparable to the cross-correlation matrix for the whole sample ($r \geq 0.84$, $p < 0.001$ in all tests). See ADNI and *COGNORM* cross-correlation matrices in Tables S3 and S4.

3.2. Effects of CSF neurodegeneration markers on brain atrophy

3.2.1. Brain atrophy over time

Linear mixed-models controlling for Age at baseline, Sex, and Cohort and random intercepts for participants, showed significant loss of HC volume (t = -28.5; $p < 0.001$) and thinning of the EC (t = -12.0; $p < 0.001$). The mean annual decline of HC volume and EC thickness was 1.15% and 0.57%, respectively. The Cohort (ADNI vs. COGNORM) was not significantly related neither to HC volume nor EC thickness at baseline or their change ($p > 0.05$).

3.2.2. Relationship between CSF biomarkers and brain atrophy: linear mixed models

Linear mixed models showed that higher NFL, FABP3, and t-tau CSF values were associated with steeper EC thinning and more HC atrophy ($p < 0.05$), while CSF Ng was unrelated to brain change. See the Biomarker and the Time × Biomarker effects detailed in Table 3. See a visual representation of the effects in Fig. 1.

3.2.3. Relationship between CSF biomarkers and brain atrophy: GAMM models

We re-ran the same model in a GAMM framework, that allows for non-linear relationships between Time, Biomarker, and Time × Biomarker and brain atrophy. See stats in Table S5. As expected, GAMMs also showed Time × Biomarker interactions for t-tau, NFL, and FABP3. However, the results also suggested most interactions showed non-linear trends such as the case of NFL and FABP3 on EC (edf = 3.15, 3.81) and NFL and t-tau on HC (edf = 3.09, 2.77). Fig. 2 for a visual representation. These trends indicate that the relationship between CSF biomarkers and accelerated brain atrophy only exists at high CSF biomarker values; approximately from values >1SD onwards. Below this threshold, variations in the CSF biomarkers were less strongly related to prospective brain atrophy.

3.3. CSF markers of Neurodegeneration and core AD biomarkers Aβ and p-tau and APOE ε4 allele

3.3.1. Is the relationship between CSF and brain integrity moderated by Amyloid-β status?

Next, we tested whether the relationship between neurodegeneration CSF biomarkers and brain atrophy was moderated by the presence of amyloid-β deposition as quantified by Aβ status. We ran linear mixed-effects models with Time, Biomarker, and Aβ status and their interactions as the effects of interest. The results did not reveal significant interaction effects of neurodegeneration CSF biomarker and Aβ status neither on brain integrity at baseline nor prospective brain atrophy ($p \geq 0.08$) (Table S6). Aβ^+ was related to more EC thinning ($p \approx 0.01$–0.05 depending on the model) but not to HC atrophy nor brain volume/ thickness at baseline ($p \geq 0.5$). See a visual representation of the results in Fig. 3.

We repeated the analysis using different Aβ status threshold criteria, that is, considering more lenient or more stringent criteria for Aβ positivity (Fig. 4). When using more lenient criteria for defining individuals as Aβ^+, we found evidence of a significant interaction between FABP3 and Aβ for predicting Entorhinal cortex thinning. Similarly, the interaction of t-tau and Aβ significantly predicted hippocampal atrophy. The remaining tests did not surpass the adjusted criteria for statistical significance. However, the patterns suggest that using more lenient criteria for defining individuals with Aβ^+ may reveal additional interactions between biomarkers when predicting brain atrophy in cognitively healthy OA.

3.3.2. Is the relationship between CSF and brain integrity moderated by the presence of the APOE ε4 allele?

Next, we tested whether the relationships between CSF and brain integrity differed between APOE ε4 carriers and non-carriers. No significant Biomarker × APOEε4 were found on entorhinal thickness or hippocampal volume ($p > 0.05$). However, t-tau × APOEε4 (p = 0.02) and Ng × APOEε4 (p = 0.03) interactions were significantly associated with hippocampal decline over time (Table S7). In both cases, APOE ε4 non-carriers with low CSF biomarker load showed less hippocampal atrophy over time. No significant Biomarker × APOEε4 × Aβ status interactions on brain atrophy were found when both APOE ε4 and Aβ status were introduced in the model ($p > 0.05$).

3.3.3. Does p-tau explain the relationship between CSF and brain atrophy?

We then tested whether the relationship between neurodegeneration CSF biomarkers and brain atrophy could be explained by the effects of p-tau on brain atrophy over time. We ran linear

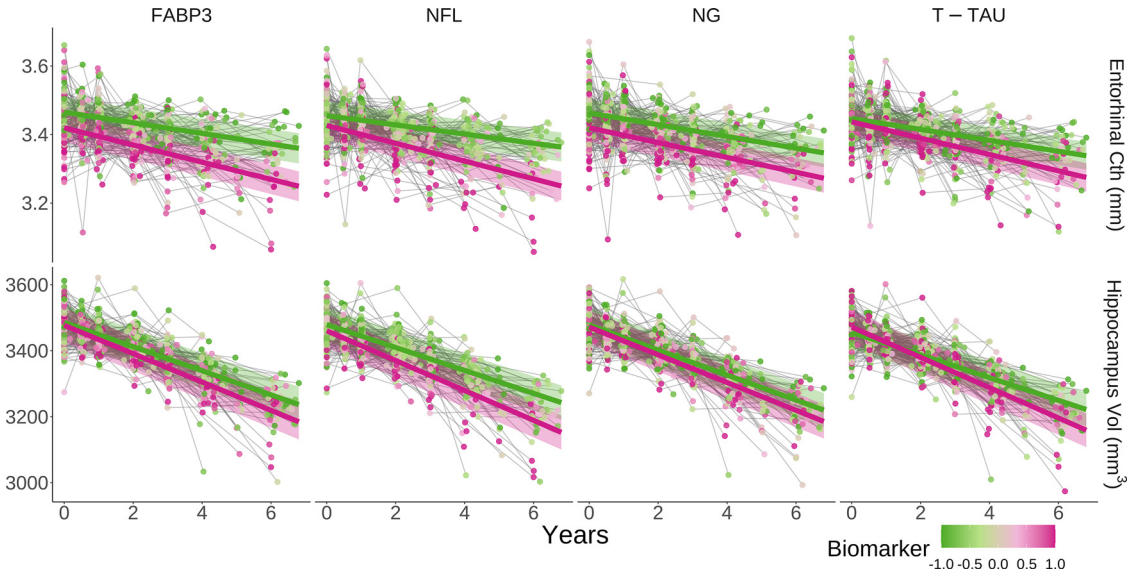

Fig. 1. Relationship between CSF biomarkers of Neurodegeneration and brain atrophy. Scaled CSF biomarkers are shown in a green-magenta scale (saturated at 1 SD). For visualizing an interaction between 2 continuous variables, we sampled the trajectories of each neurodegeneration CSF biomarker on brain values – as a function of time - at mean CSF ±1 SD using the predict function (green/magenta = -1 SD/+1 SD, i.e., low/high CSF values). Points represent single observations united within participants by grey lines. Observations are adjusted by the covariates of no-interest and the participant-identifier fixed effects. Ribbons reflect standard errors of the mean (SEM). Abbreviations: NFL, Neurofilament light; NG, Neurogranin; FABP3, Heart-type fatty acid-binding protein 3; Cth, Cortical Thickness; Vol, Volume. See Table 3 for stats. (For interpretation of the references to color in this figure legend, the reader is referred to the Web version of this article.)

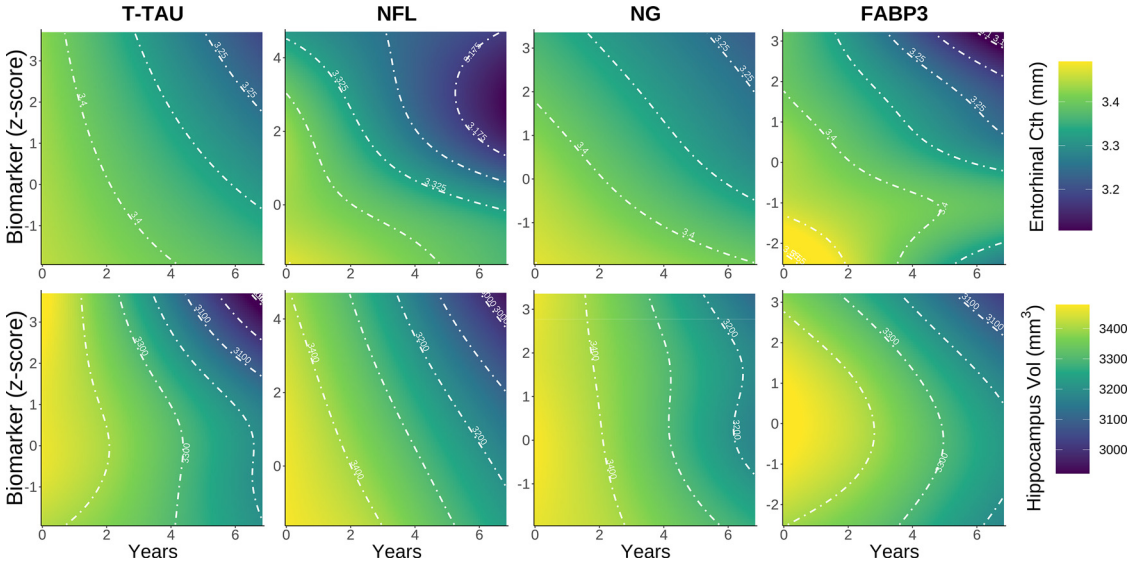

Fig. 2. GAMM fits; Time × Biomarker interactions on brain atrophy. The figure shows the Time (x-axis) × CSF biomarker (y-axis; scaled) interaction on Entorhinal thickness (upper panels) and Hippocampal volume (lower panels) shown on the z-axis as a yellow-green-blue scale. Abbreviations: NFL, Neurofilament light; NG, Neurogranin; FABP3, Heart-type fatty acid-binding protein 3; Cth, Cortical Thickness; Vol, Volume. White lines were drawn as contours for illustrative purposes. See stats in Table S5. (For interpretation of the references to color in this figure legend, the reader is referred to the Web version of this article.)

mixed-effects models as described above additionally controlling for p-tau and Time × p-tau effects. The relationships between CSF NFL with both EC thinning and HC atrophy remained significant when controlling for p-tau effects (EC: t = -3.27, p = 0.001; HC: t = -2.91, p = 0.004). CSF FABP3 was also significantly associated with EC thinning (t = -1.98, p = 0.05) when controlling for p-tau. The remaining comparisons were not statistically significant (p > 0.25) except in the case of CSF Ng, which predicted preservation of HC volume over time (p = 0.009). See full stats in Table S8.

3.3.4. LASSO feature selection: When combined, which biomarkers better predict brain atrophy?

Finally, we used a LASSO algorithm to select the CSF biomarkers that best predicted hippocampal atrophy and entorhinal cortical thinning. We used Age, Sex, the AD biomarkers Aβ and p-tau, and the 4 CSF biomarkers of neurodegeneration as variables of interest. An optimal λ = 1.28 for EC and 2.70 for HC predictions were first defined using cross-validation. The optimal model for EC thinning included Age, t-tau and NFL as predictors (β = -0.80^{-3}, -0.73^{-3}, -2.50^{-3} mm). The optimal model for HC atrophy

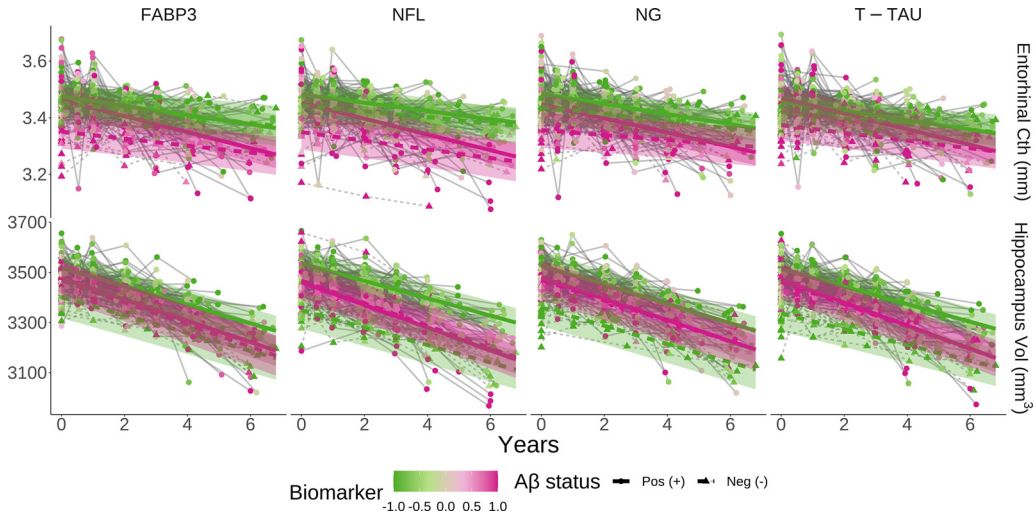

Fig. 3. Interaction between CSF biomarkers of Neurodegeneration and Aβ42 on brain atrophy. Scaled CSF biomarkers are shown in a green-magenta scale (saturated at 1 SD). Aβ+/Aβ− status is shown as dashed and/or solid lines and triangles and/or circles. For visualizing an interaction between 2 continuous variables, we sampled the trajectories of each neurodegeneration CSF biomarker on brain values – as a function of time - at mean CSF ±1 SD using the predict function (green/magenta = -1 SD/+1 SD, i.e., low/high CSF values). Points represent single observations united within participants by grey lines. Observations are adjusted by the covariates of no-interest and the participant-identifier fixed effects. Ribbons reflect standard errors of the mean (SEM). Abbreviations: NFL, Neurofilament light; NG, Neurogranin; FABP3, Heart-type fatty acid-binding protein 3; Cth, Cortical Thickness; Vol, Volume. See Table S6 for stats. (For interpretation of the references to color in this figure legend, the reader is referred to the Web version of this article.)

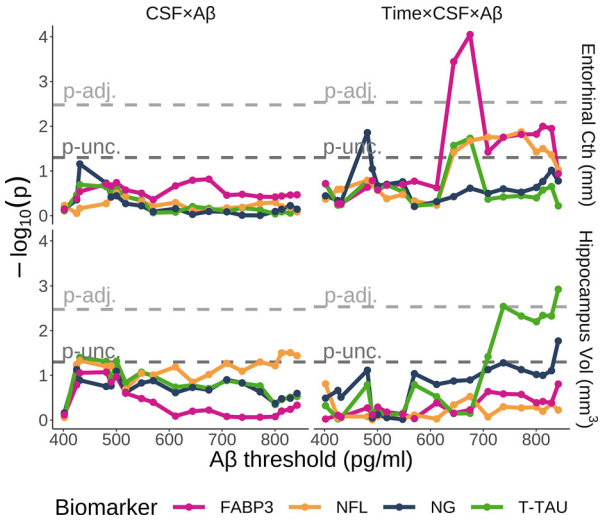

Fig. 4. Effects of varying Aβ42 threshold positivity on brain integrity. *p*-values for Time × Biomarker × Aβ and Biomarker × Aβ on Entorhinal Cortex thickness and Hippocampal volume using different criteria for defining individuals with positive Aβ status. p-unc = 0.05, p-adj ≈ 0.003 (Bonferroni-like adjustment). Abbreviations: NFL, Neurofilament light; NG, Neurogranin; FABP3, Heart-type fatty acid-binding protein 3; CSF, Cerebrospinal fluid; Cth, Cortical Thickness; Vol, Volume.

included Age, Aβ, t-tau, NFL, and FABP3 as independent predictors (β = -0.62, 4.02, -2.77, -2.09 mm^3). Note that β-coefficients represent annualized change and the model's selection of t-tau over p-tau is possibly arbitrary due to their high correlation.

3.4. Are spatial patterns of CSF biomarker-related cortical thinning related to gene expression of specific cellular components?

3.4.1. Spatial patterns of CSF biomarker-related cortical thinning

First, we obtained the cortical signatures of the different CSF biomarkers of neurodegeneration by extending the main analysis to the n = 34 bilateral ROIs. See the relationship between CSF biomarkers and cortical thinning in Fig. 5A. For completeness, we repeated the analyses using Aβ as moderator and controlling for p-tau (Fig. S2). The spatial correlation amongst biomarker-related cortical thinning is shown in Fig. 5B.

3.4.2. Spatial patterns of CSF biomarker-related cortical thinning relate to gene expression patterns for specific cellular components

Finally, to shed light on the biological substrates underpinning cortical thinning in each biomarker, we compared the spatial signatures of cortical decline associated with each biomarker with the spatial patterns of gene expression associated with specific cellular components. The pattern of cortical thinning associated with baseline t-tau resembled most those of genes expressed in the *axonal growth cone* (r = -0.50, p_{unc} = 0.002, n_{genes} = 27), the *AMPA glutamate receptor complex* (r = -0.50, p_{unc} = 0.002, n_{genes} = 24), the *neurotransmitter receptor complex* (r = -0.47, p_{unc} = 0.003, n_{genes} = 47), and the *excitatory synapse* (r = -0.46, p_{unc} = 0.004, n_{genes} = 44). For NFL, genes expressed in the cortical cytoskeleton (r = -0.61, p_{fdr} < 0.001, n_{genes} = 86), the *cortical actin cytoskeleton* (r = -0.60, p_{fdr} = 0.005, n_{genes} = 64), and the Ruffle membrane (r = -0.57, p_{fdr} = 0.006, n_{genes} = 84) were the most strongly associated with the spatial patterns of cortical thinning. For Ng, genes expressed in the *dendritic shaft* (r = -0.40, p_{unc} < 0.009, n_{genes} = 31) were the most strongly associated with the spatial patterns of cortical thinning. Finally, for FABP3, genes expressed in the *RNA polymerase II holoenzyme* (r = -0.53, p_{unc} < 0.001, n_{genes} = 68), the *rough endoplasmatic reticulum membrane* (r = -0.48, p_{unc} = 0.003, n_{genes} = 25), the *anaphase promoting complex* (r = -0.48, p_{fdr} = 0.003, n_{genes} = 20), and the *triglyceride rich plasma lipoprotein particle* (r = -0.46, p_{fdr} = 0.004, n_{genes} = 11) were amongst the most strongly associated with the spatial patterns of cortical thinning. See top terms in Fig. S3. In summary, the patterns of cortical thinning associated with the CSF biomarkers of neurodegeneration overlap with genes expressed in specific cellular components, which grossly match the putative biological substrates of the biomarkers (e.g., for t-tau axonal damage and excitatory neurons, for NFL compromised cytoskeleton, Ng as marker of postsynaptic function, and FABP3 as a marker of lipid dyshomeostasis). Note that due to stringent multiple comparison correction, corrected results are only found for the NFL patterns.

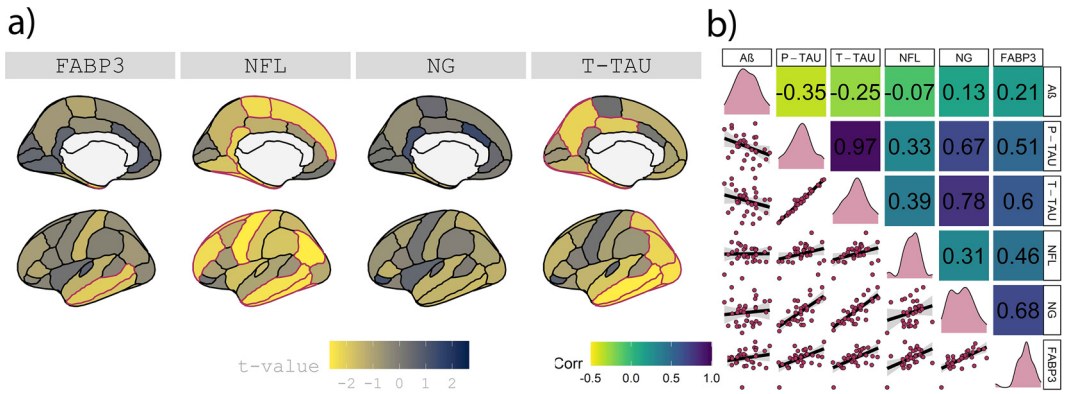

Fig. 5. Relationship between CSF biomarkers of Neurodegeneration and cortical thinning. (A) Effects of CSF biomarkers on cortical thinning (Time × Biomarker effect) shown in a blue-brown-yellow scale where yellow represents steeper thinning with higher levels of the biomarker. For visualization purposes, ROIs with effects $p < 0.05$ are drawn with red lines. (B) Spatial correlation between CSF biomarker-related maps of cortical thinning. The upper triangular matrix shows the Spearman (ρ) correlation between cortical maps. The lower triangular matrix displays the same correlation using a scatter plot where each point represents the t-value for a unique cortical region. The diagonal shows the probability density function for each CSF biomarker. That is, for each biomarker, it shows the distribution of the effects (t-values) throughout all the cortical regions. Abbreviations: NFL, Neurofilament light; NG, Neurogranin; FABP3, Heart-type fatty acid-binding protein 3. (For interpretation of the references to color in this figure legend, the reader is referred to the Web version of this article.)

4. Discussion

The results showed that the neurodegeneration biomarkers NFL, t-tau, and FABP3 - but not Ng - predicted both HC atrophy and thinning of the EC. The association of NFL - and to a lesser degree, FABP3 - with brain atrophy was not moderated by Aβ42 nor explained by p-tau. The patterns of cortical thinning corresponding to each CSF biomarker were related to distinct neurogenetic profiles associated with specific cellular substrates such as axonal or dendritic components. The implications of these findings are discussed below.

4.1. NFL is related to brain atrophy in cognitively healthy older adults regardless of amyloid and tau pathology

The relationship between NFL and brain atrophy in aging, and its independence from amyloid and tau pathology biomarkers, fits well with the existing literature (Hansson, 2021). Increased levels of NFL in both CSF and blood are found with higher age - even when controlling for concomitant neurodegenerative diseases (Idland et al., 2017; Khalil et al., 2018; Vågberg et al., 2015). Variations in baseline NFL often relate to the slope of brain atrophy and cognitive decline in many conditions such as AD, frontotemporal dementia, and vascular disease (Egle et al., 2021; Mattsson et al., 2017; Rohrer et al., 2016) but also in cognitively healthy OA samples (Idland et al., 2017; Khalil et al., 2020). Further, longitudinal change in plasma NFL parallels brain changes both in cognitively healthy OA (Khalil et al., 2020), and AD patients (Mattsson et al., 2019) while reductions in NFL are associated with treatment effectiveness in several diseases (Olsson et al., 2019). Overall, our results indicate that cross-sectional CSF NFL is a good predictor of brain atrophy in cognitively healthy OA, capturing relatively unspecific accumulation of diverse subclinical - and preclinical - brain damage related to axonal alterations (Khalil et al., 2018). The neurodegenerative mechanisms behind increased NFL in cognitively healthy OA are unclear, however, they most likely overlap with those underlying specific diseases to some degree. Top candidate etiologies are cerebrovascular pathology (Nyberg et al., 2020) and tau-related damage (Mattsson et al., 2019). It is uncertain whether NFL captures *normal* age-related myelin alterations (Peters and Sethares, 2002) as they do not include extensive axonal degeneration. One speculation is that CSF NFL in cognitively healthy OA relates to decreased neurofilament phosphorylation, which renders axonal neurofilament more vulnerable to breakdown (de Waegh et al., 1992). The neurogenetic analysis pointed in this direction as NFL-related cortical thinning overlapped with the topography of genes expressed in the cytoskeleton. This is in agreement with NFL being a key protein in the neural cytoskeleton, a marker of neuroaxonal damage in CSF (Khalil et al., 2018; Lépinoux-Chambaud and Eyer, 2013), and evidence that myelination contributes strongly to the T1-weighted signal (Eickhoff et al., 2005). Considering NFL can also be reliably quantified in blood, this biomarker has substantial clinical utility as it can detect ongoing neurodegenerative changes in cognitively healthy individuals. In combination with other biomarkers, it can improve predictions and select individuals with a higher risk of future cognitive decline.

4.2. FABP3 relates to brain atrophy in cognitively healthy older adults and is partially independent of core AD biomarkers

CSF FABP3 was also associated with brain atrophy in the EC and this relationship remained significant when controlling for levels of p-tau. The literature on FABP3 in aging and dementia is still scarce. Here, we provide first-time evidence of a relationship between temporal lobe atrophy and FABP3 in cognitively healthy older adults. Using ADNI, FABP3 has been associated with atrophy of EC and other AD-vulnerable regions in a previous study that included both demented and non-demented individuals (Desikan et al., 2013). This relationship was moderated by Aβ status, and only individuals with low CSF Aβ and high levels of FABP3 showed steeper cortical thinning. Using a clustering approach with the COGNORM dataset, Idland and colleagues (2020) found that individuals with high tau, p-tau, and FABP3 levels showed more temporal lobe atrophy independently of Aβ levels. Similarly, our results did not support Aβ as a moderator of the relationship between FABP3 and brain atrophy, though ultimately this interaction might be dependent on the threshold for defining Aβ status and the presence of dementia. Interestingly though, FABP3 often emerges as a relevant biomarker in machine learning approaches in the context of aging and neurodegenerative diseases. For example, FABP3 was a top biomarker for predicting AD (O'Bryant et al., 2013), was an important predictor of conversion and diagnostic accuracy (Chiasserini et al., 2017), and appeared as the most abnormal CSF biospecimen in the healthy aging-AD continuum (Iturria-Medina et al., 2016). These findings align with our feature selection results showing FABP3 as an independent contributor to hip-

pocampal decline. The source of FABP3 in CSF in older individuals is still uncertain but has been interpreted as reflecting vascular dysregulation, metabolic integrity, membrane integrity, and cell dysfunction. In the brain, FABP3 is involved in the transport of fatty acids and thus plays a role in maintaining neuronal membrane integrity, neurite growth, and synapse formation (Janssen and Kiliaan, 2014). The neurogenetic analyses suggested that FABP3-related cortical thinning captures *primary* loss of lipid integrity and/or *downstream* effects mediated by fatty acid control of gene expression (Pégorier et al., 2004). The results suggest FABP3 can capture brain decline in cognitively healthy OA that is partly independent of pathological processes associated with AD.

4.3. Ng and t-tau do not relate to brain atrophy in cognitively healthy older adults independently from core AD biomarkers

CSF levels of Neurogranin (Ng) were unrelated to brain atrophy. Associations of Ng with brain integrity have only been observed in previous studies using ADNI data in individuals with Aβ pathology or presenting MCI (Pereira et al., 2017; Portelius et al., 2015). Likewise, abnormal Ng levels are seen both in undemented Aβ^+ and MCI individuals (Pereira et al., 2021; Portelius et al., 2015), but are normal in most neurodegenerative conditions, suggesting that Ng reflects AD-specific post-synaptic dysfunction. In a community-based sample, Ng levels were elevated in Aβ^+ individuals but otherwise were largely unrelated to cognitive function and health status (age and sex-adjusted) (Mielke et al., 2019). Our findings are thus in line with this literature suggesting that, while Ng is a useful marker of neurodegeneration in early AD, it is not a (very) sensitive biomarker of brain atrophy in non-demented populations. The neurogenetic analyses suggest a relationship between Neurogranin-related cortical thinning and post-synaptic dysfunction - as associated with genes expressed in the dendritic shaft - in agreement with existing literature.

We considered t-tau as a marker of neurodegeneration as it is unspecific to AD and is high in other neurodegenerative diseases and brain conditions (Hansson, 2021; Jack et al., 2018). The results, however, showed a high correlation between p-tau and t-tau and that t-tau-related brain atrophy was not independent of p-tau. Thus, we conclude that in the context of cognitively healthy aging, p-tau and t-tau are mostly interchangeable and t-tau-related brain atrophy is closely linked to tau-phosphorylation. The neurogenetic analyses showed t-tau-related cortical thinning was associated with gene expression in the axonal part (*axonal growth cone*) consistent with tau proteins being a key structural and functional element of axons. The relationship of both t-tau and Ng was moderated by the presence of – at least, 1 – APOE ε4 allele. These results suggest that in cognitively healthy OA both biomarkers may inform on brain changes that are often associated with AD pathology and are in line with the notion of APOE ε4 being a key for understanding neuropathological variability in OA and AD (Frisoni et al., 2022).

4.4. Limitations and technical considerations

Several limitations and technical aspects associated with this study need to be addressed. The sample in the present study had idiosyncratic characteristics due to (1) the inclusion of older adults that remained cognitively healthy during follow-up, and (2) the combination of the COGNORM and ADNI cohorts. Selection bias is a well-known concern and an inherent problem in aging studies (Hardy et al., 2009). Individuals need to survive and be healthy enough to satisfy inclusion criteria up until old age and, in longitudinal studies, come back repeatedly for follow-up testing. The decision of excluding converters was motivated by the need to understand the trajectories of brain atrophy in relation to CSF biomarkers in cognitively healthy older individuals. The development of reliable markers of neurodegeneration in this population is key for early prediction and early therapeutic interventions before the presence of widespread brain and cognitive decline. Yet, this decision increased sample bias towards a "healthy(ier) volunteer" profile. The different composition of samples across studies is likely an important factor in explaining the heterogeneity of the results. To consider here is a non-significant interaction between t-tau and Aβ status on longitudinal brain atrophy. It is possible that the inclusion of participants closer to cognitive decline, which – on average - would present low CSF Aβ, high CSF t-tau (and NG), and steep atrophy, would have caused this interaction to be significant.

Here we combined 2 different samples of cognitively healthy OA to increase power. Combining different cohorts may create new sources of error due to differences in the populations or the measurements (Zuo et al., 2019). Here, differences in recruitment, CSF collection procedures, MRI acquisition sequences, and duration of the follow-up are potential sources of systematic noise. To minimize this problem, we scaled the CSF biomarkers within each cohort and introduced cohort as a covariate in all analyses. While the cohorts differed in the proportion of Aβ^+ and APOE ε4 carriers, they showed comparable rates of brain atrophy and a similar structure of correlation between biomarkers. The emergence of several other independent datasets characterized by available CSF - and plasma - biomarkers at baseline and longitudinal MRI observations will enable reliability testing in future work. Finally, we must highlight that the correlational nature of the analyses does not warrant causality or directionality claims. While the inclusion of prospective longitudinal MRI data provides a greater degree of confidence, the constrain is especially poignant in the neurogenetic analyses. The spatial correlations cannot differentiate between *upstream* and *downstream* effects, nor one can fully exclude the impact of unaccounted variables.

5. Conclusions

This study sheds light on the relationship between baseline CSF biomarkers and prospective longitudinal decline in cognitively healthy older individuals with a relatively low burden of neurodegeneration. We found that NFL and FABP3 predict brain atrophy independently of biomarkers for brain amyloidosis and tau pathology. Since these biomarkers reflect partially different biological processes, we suggest that in combination they can improve the accuracy of individual predictions of brain atrophy and its topography in cognitively healthy older adults.

Verification

This article describes original work that is not under consideration for publication elsewhere. The publication is approved by all authors and tacitly or explicitly by the responsible authorities where the work was carried out. If this article will be accepted, it will not be published elsewhere in any form.

Disclosure Statements

HZ has served on scientific advisory boards and/or as a consultant for Abbvie, Alector, Eisai, Denali, Roche Diagnostics, Wave, Samumed, Siemens Healthineers, Pinteon Therapeutics, Nervgen, AZTherapies, CogRx, and Red Abbey Labs; has given lectures in symposia sponsored by Cellectricon, Fujirebio, Alzecure, and Biogen, and is a co-founder of Brain Biomarker Solutions in Gothenburg AB (BBS), which is a part of the GU Ventures Incubator Program. KB has served as a consultant, at advisory boards,

or on data monitoring committees for Abcam, Axon, Biogen, JOMDD/Shimadzu. Julius Clinical, Lilly, MagQu, Novartis, Prothena, Roche Diagnostics, and Siemens Healthineers, and is a co-founder of Brain Biomarker Solutions in Gothenburg AB (BBS), which is a part of the GU Ventures Incubator Program. All conflicts of interest are unrelated to the work presented in this paper.

Acknowledgements

This work was supported by the Department of Psychology, University of Oslo (to K.B.W., A.M.F.), the Norwegian Research Council (to K.B.W., A.M.F., D.V.P. (ES694407)) and the project has received funding from the European Research Council's Starting Grant scheme under grant agreements 283634, 725025 (to A.M.F.) and 313440 (to K.B.W.). L.O.W. and data collection in COGNORM is funded by the South-Eastern Norway Regional Health Authorities (grant number 2017095) and The Norwegian Health Association. HZ is a Wallenberg Scholar supported by grants from the Swedish Research Council (2018-02532), the European Research Council (681712), Swedish State Support for Clinical Research (ALFGBG-720931), the Alzheimer Drug Discovery Foundation (ADDF), USA (201809-2016862), the AD Strategic Fund and the Alzheimer's Association (ADSF-21-831376-C, ADSF-21-831381-C and ADSF-21-831377-C), the Olav Thon Foundation, the Erling-Persson Family Foundation, Stiftelsen för Gamla Tjänarinnor, Hjärnfonden, Sweden (FO2019-0228), the European Union's Horizon 2020 research and innovation programme under the Marie Skłodowska-Curie grant agreement No 860197 (MIRIADE), and the UK Dementia Research Institute at UCL. KB is supported by the Swedish Research Council (2017-00915), the Alzheimer Drug Discovery Foundation (ADDF), USA (RDAPB-201809-2016615), the Swedish Alzheimer Foundation (AF-742881), Hjärnfonden, Sweden (FO2017-0243), the Swedish state under the agreement between the Swedish government and the County Councils, the ALF-agreement (ALFGBG-715986), the European Union Joint Program for Neurodegenerative Disorders (JPND2019-466-236), the National Institute of Health (NIH), USA, (grant 1R01AG068398-01), and the Alzheimer's Association 2021 Zenith Award (ZEN-21-848495). Data collection and sharing for this project were funded by the ADNI (NIH Grant U01 AG024904) and DOD ADNI (Department of Defense award number W81XWH-12-2-0012). ADNI is funded by the National Institute on Aging, the National Institute of Biomedical Imaging and Bioengineering, and through generous contributions from the following: AbbVie, Alzheimer's Association; Alzheimer's Drug Discovery Foundation; Araclon Biotech; BioClinica, Inc.; Biogen; Bristol-Myers Squibb Company; CereSpir, Inc.; Cogstate Eisai Inc.; Elan Pharmaceuticals, Inc.; Eli Lilly and Company; EuroImmun; F. Hoffmann-La Roche Ltd and its affiliated company Genentech, Inc.; Fujirebio; GE Healthcare; IXICO Ltd.; Janssen Alzheimer Immunotherapy Research & Development, LLC.; Johnson & Johnson Pharmaceutical Research & Development LLC.; Lumosity; Lundbeck; Merck & Co., Inc.; Meso Scale Diagnostics, LLC.; NeuroRx Research; Neurotrack Technologies; Novartis Pharmaceuticals Corporation; Pfizer Inc.; Piramal Imaging; Servier; Takeda Pharmaceutical Company; and Transition Therapeutics. The Canadian Institutes of Health Research is providing funds to support ADNI clinical sites in Canada. Private sector contributions are facilitated by the Foundation for the National Institutes of Health (http://www.fnih.org). The grantee organization is the Northern California Institute for Research and Education, and the study is coordinated by the Alzheimer's Therapeutic Research Institute at the University of Southern California. ADNI data are disseminated by the Laboratory for Neuro Imaging at the University of Southern California.

Supplementary materials

Supplementary material associated with this article can be found, in the online version, at doi:10.1016/j.neurobiolaging.2022.04.010.

CRediT authorship contribution statement

Didac Vidal-Piñeiro: Conceptualization, Formal analysis, Visualization, Writing – original draft. **Øystein Sørensen:** Formal analysis, Methodology. **Kaj Blennow:** Formal analysis, Software, Resources. **Elettra Capogna:** Visualization, Data curation. **Nathalie Bodd Halaas:** Data curation, Investigation, Resources. **Ane-Victoria Idland:** Data curation, Investigation, Resources. **Athanasia Monica Mowinckel:** Formal analysis, Software. **Joana Braga Pereira:** Conceptualization. **Leiv Otto Watne:** Funding acquisition, Conceptualization, Investigation, Data curation. **Henrik Zetterberg:** Formal analysis, Software, Resources. **Kristine Beate Walhovd:** Funding acquisition, Conceptualization. **Anders Martin Fjell:** Funding acquisition, Supervision, Conceptualization.

References

Bittner, T., Zetterberg, H., Teunissen, C.E., Ostlund, R.E., Militello, M., Andreasson, U., Hubeek, I., Gibson, D., Chu, D.C., Eichenlaub, U., Heiss, P., Kobold, U., Leinenbach, A., Madin, K., Manuilova, E., Rabe, C., Blennow, K., 2016. Technical performance of a novel, fully automated electrochemiluminescence immunoassay for the quantitation of β-amyloid (1-42) in human cerebrospinal fluid. Alzheimers Dement 12, 517–526. doi:10.1016/j.jalz.2015.09.009.

Boyle, P.A., Wang, T., Yu, L., Wilson, R.S., Dawe, R., Arfanakis, K., Schneider, J.A., Bennett, D.A., 2021. To what degree is late life cognitive decline driven by age-relatedneuropathologies? Brain doi:10.1093/brain/awab092.

Boyle, P.A., Yu, L., Wilson, R.S., Leurgans, S.E., Schneider, J.A., Bennett, D.A., 2018. Person-specific contribution of neuropathologies to cognitive loss in old age. Ann Neurol 83, 74–83. doi:10.1002/ana.25123.

Bridel, C., van Wieringen, W.N., Zetterberg, H., Tijms, B.M., Teunissen, C.E., Group, the NFL, Alvarez-Cermeño, J.C., Andreasson, U., Axelsson, M., Bäckström, D.C., Bartos, A., Bjerke, M., Blennow, K., Boxer, A., Brundin, L., Burman, J., Christensen, T., Fialová, L., Forsgren, L., Frederiksen, J.L., Gisslén, M., Gray, E., Gunnarsson, M., Hall, S., Hansson, O., Herbert, M.K., Jakobsson, J., Jessen-Krut, J., Janelidze, S., Johannsson, G., Jonsson, M., Kappos, L., Khademi, M., Khalil, M., Kuhle, J., Landén, M., Leinonen, V., Logroscino, G., Lu, C.-H., Lycke, J., Magdalinou, N.K., Malaspina, A., Mattsson, N., Meeter, L.H., Mehta, S.R., Modvig, S., Olsson, T., Paterson, R.W., Pérez-Santiago, J., Piehl, F., Pijnenburg, Y.A.L., Pyykkö, O.T., Ragnarsson, O., Rojas, J.C., 2019. Diagnostic value of cerebrospinal fluid neurofilament light protein in neurology: a systematic review and meta-analysis. JAMA Neurol doi:10.1001/jamaneurol.2019.1534.

Burt, J.B., Helmer, M., Shinn, M., Anticevic, A., Murray, J.D., 2020. Generative modeling of brain maps with spatial autocorrelation. Neuroimage 220, 117038. doi:10.1016/j.neuroimage.2020.117038.

Chiasserini, D., Biscetti, L., Eusebi, P., Salvadori, N., Frattini, G., Simoni, S., Roeck, N.D., Tambasco, N., Stoops, E., Vanderstichele, H., Engelborghs, S., Mollenhauer, B., Calabresi, P., Parnetti, L., 2017. Differential role of CSF fatty acid binding protein 3, α-synuclein, and Alzheimer's disease core biomarkers in Lewy body disorders and Alzheimer's dementia. Alz Res Therapy 9, 1–12. doi:10.1186/s13195-017-0276-4.

Dale, A.M., Fischl, B., Sereno, M.I., 1999. Cortical surface-based analysis. I. Segmentation and surface reconstruction. Neuroimage 9, 179–194. doi:10.1006/nimg.1998.0395.

de Waegh, S.M., Lee, V.M., Brady, S.T., 1992. Local modulation of neurofilament phosphorylation, axonal caliber, and slow axonal transport by myelinating Schwann cells. Cell 68, 451–463. doi:10.1016/0092-8674(92)90183-d.

DeKosky, S.T., Golde, T., 2016. Cerebrospinal biomarkers in alzheimer disease—potential roles as markers of prognosis and neuroplasticity. JAMA Neurol 73, 508–510. doi:10.1001/jamaneurol.2016.0090.

Desikan, R.S., Ségonne, F., Fischl, B., Quinn, B.T., Dickerson, B.C., Blacker, D., Buckner, R.L., Dale, A.M., Maguire, R.P., Hyman, B.T., Albert, M.S., Killiany, R.J., 2006. An automated labeling system for subdividing the human cerebral cortex on MRI scans into gyral based regions of interest. Neuroimage 31, 968–980. doi:10.1016/j.neuroimage.2006.01.021.

Desikan, R.S., Thompson, W.K., Holland, D., Hess, C.P., Brewer, J.B., Zetterberg, H., Blennow, K., Andreassen, O.A., McEvoy, L.K., Hyman, B.T., Dale, A.M., 2013. Heart fatty acid binding protein and Aβ-associated Alzheimer's neurodegeneration. Mol Neurodegener 8, 39. doi:10.1186/1750-1326-8-39.

Dhiman, K., Blennow, K., Zetterberg, H., Martins, R.N., Gupta, V.B., 2019. Cerebrospinal fluid biomarkers for understanding multiple aspects of Alzheimer's disease pathogenesis. Cell. Mol. Life Sci. 76, 1833–1863. doi:10.1007/s00018-019-03040-5.

Díez-Guerra, F.J., 2010. Neurogranin, a link between calcium/calmodulin and protein kinase C signaling in synaptic plasticity. IUBMB Life 62, 597–606. doi:10.1002/iub.357.

Egle, M., Loubiere, L., Maceski, A., Kuhle, J., Peters, N., Markus, H.S., 2021. Neurofilament light chain predicts future dementia risk in cerebral small vessel disease. J Neurol Neurosurg Psychiatry 92, 582–589. doi:10.1136/jnnp-2020-325681.

Eickhoff, S., Walters, N.B., Schleicher, A., Kril, J., Egan, G.F., Zilles, K., Watson, J.D.G., Amunts, K., 2005. High-resolution MRI reflects myeloarchitecture and cytoarchitecture of human cerebral cortex. Hum Brain Mapp 24, 206–215. doi:10.1002/hbm.20082.

Fischl, B., Sereno, M.I., Dale, A.M., 1999. Cortical surface-based analysis. II: Inflation, flattening, and a surface-based coordinate system. Neuroimage 9, 195–207. doi:10.1006/nimg.1998.0396.

Folstein, M.F., Folstein, S.E., McHugh, P.R., 1975. "Mini-mental state". A practical method for grading the cognitive state of patients for the clinician. J Psychiatr Res 12, 189–198.

Frisoni, G.B., Altomare, D., Thal, D.R., Ribaldi, F., van der Kant, R., Ossenkoppele, R., Blennow, K., Cummings, J., van Duijn, C., Nilsson, P.M., Dietrich, P.-Y., Scheltens, P., Dubois, B., 2022. The probabilistic model of Alzheimer disease: the amyloid hypothesis revised. Nat Rev Neurosci 23, 53–66. doi:10.1038/s41583-021-00533-w.

Gangishetti, U., Christina Howell, J., Perrin, R.J., Louneva, N., Watts, K.D., 2018. Non-beta-amyloid/tau cerebrospinal fluid markers inform staging and progression in Alzheimer's disease. Alzheimers Res Ther 10, 98. doi:10.1186/s13195-018-0426-3.

Gattringer, T., Pinter, D., Enzinger, C., Seifert-Held, T., Kneihsl, M., Fandler, S., Pichler, A., Barro, C., Gröbke, S., Voortman, M., Pirpamer, L., Hofer, E., Ropele, S., Schmidt, R., Kuhle, J., Fazekas, F., Khalil, M., 2017. Serum neurofilament light is sensitive to active cerebral small vessel disease. Neurology 89, 2108–2114. doi:10.1212/WNL.0000000000004645.

Gorbach, T., Pudas, S., Lundquist, A., Orädd, G., Josefsson, M., Salami, A., de Luna, X., Nyberg, L., 2017. Longitudinal association between hippocampus atrophy and episodic-memory decline. Neurobiol. Aging 51, 167–176. doi:10.1016/j.neurobiolaging.2016.12.002.

Groot, C., Grothe, M.J., Mukherjee, S., Jelistratova, I., Jansen, I., van Loenhoud, A.C., Risacher, S.L., Saykin, A.J., 2021. Differential patterns of gray matter volumes and associated gene expression profiles in cognitively-defined Alzheimer's disease subgroups. NeuroImage: Clinical 30, 102660. doi:10.1016/j.nicl.2021.102660.

Hampel, H., Blennow, K., Shaw, L.M., Hoessler, Y.C., Zetterberg, H., Trojanowski, J.Q., 2010. Total and phosphorylated tau protein as biological markers of Alzheimer's disease. Exp. Gerontol. 45, 30–40. doi:10.1016/j.exger.2009.10.010.

Hansson, O., 2021. Biomarkers for neurodegenerative diseases. Nat Med 27, 954–963. doi:10.1038/s41591-021-01382-x.

Hansson, O., Seibyl, J., Stomrud, E., Zetterberg, H., Trojanowski, J.Q., Bittner, T., Lifke, V., Corradini, V., Eichenlaub, U., Batrla, R., Buck, K., Zink, K., Rabe, C., Blennow, K., Shaw, L.M., 2018. CSF biomarkers of Alzheimer's disease concord with amyloid-β PET and predict clinical progression: A study of fully automated immunoassays in BioFINDER and ADNI cohorts. Alzheimers Dement 14, 1470–1481. doi:10.1016/j.jalz.2018.01.010.

Hardy, S.E., Allore, H., Studenski, S.A., 2009. Missing data: a special challenge in aging research. J Am Geriatr Soc 57, 722–729. doi:10.1111/j.1532-5415.2008.02168.x.

Hawrylycz, M.J., Lein, E.S., Guillozet-Bongaarts, A.L., Shen, E.H., Ng, L., Miller, J.A., van de Lagemaat, L.N., Smith, K.A., Ebbert, A., Riley, Z.L., Abajian, C., Beckmann, C.F., Bernard, A., Bertagnolli, D., Boe, A.F., Cartagena, P.M., Chakravarty, M.M., Chapin, M., Chong, J., Dalley, R.A., 2012. An anatomically comprehensive atlas of the adult human brain transcriptome. Nature 489, 391–399. doi:10.1038/nature11405.

Hill, D.L.G., Schwarz, A.J., Isaac, M., Pani, L., Vamvakas, S., Hemmings, R., Carrillo, M.C., Yu, P., Sun, J., Beckett, L., Boccardi, M., Brewer, J., Brumfield, M., Cantillon, M., Cole, P.E., Fox, N., Frisoni, G.B., Jack, C., Kelleher, T., Luo, F., Novak, G., Maguire, P., Meibach, R., Patterson, P., Bain, L., Sampaio, C., Raunig, D., Soares, H., Suhy, J., Wang, H., Wolz, R., Stephenson, D., 2014. Coalition against major diseases/european medicines agency biomarker qualification of hippocampal volume for enrichment of clinical trials in predementia stages of alzheimer's disease. Alzheimers Dement 10, 421–429. doi:10.1016/j.jalz.2013.07.003, e3doi:.

Idland, A.-V., Sala-Llonch, R., Borza, T., Watne, L.O., Wyller, T.B., Brækhus, A., Zetterberg, H., Blennow, K., Walhovd, K.B., Fjell, A.M., 2017. CSF neurofilament light levels predict hippocampal atrophy in cognitively healthy older adults. Neurobiol. Aging 49, 138–144. doi:10.1016/j.neurobiolaging.2016.09.012.

Idland, A.-V., Sala-Llonch, R., Watne, L.O., Brækhus, A., Hansson, O., Blennow, K., Zetterberg, H., Sørensen, Ø., Walhovd, K.B., Wyller, T.B., Fjell, A.M., 2020. Biomarker profiling beyond amyloid and tau: cerebrospinal fluid markers, hippocampal atrophy, and memory change in cognitively unimpaired older adults. Neurobiol. Aging 93, 1–15. doi:10.1016/j.neurobiolaging.2020.04.002.

Iturria-Medina, Y., Sotero, R.C., Toussaint, P.J., Mateos-Pérez, J.M., Evans, A.C., 2016. Early role of vascular dysregulation on late-onset Alzheimer's disease based on multifactorial data-driven analysis. Nat Commun 7, 11934. doi:10.1038/ncomms11934.

Jack, C.R., Bennett, D.A., Blennow, K., Carrillo, M.C., Dunn, B., Haeberlein, S.B., Holtzman, D.M., Jagust, W., Jessen, F., Karlawish, J., Liu, E., Molinuevo, J.L., Montine, T., Phelps, C., Rankin, K.P., Rowe, C.C., Scheltens, P., Siemers, E., Snyder, H.M., Sperling, R., 2018. NIA-AA Research Framework: Toward a biological definition of Alzheimer's disease. Alzheimers Dement 14, 535–562. doi:10.1016/j.jalz.2018.02.018.

Janssen, C.I.F., Kiliaan, A.J., 2014. Long-chain polyunsaturated fatty acids (LCPUFA) from genesis to senescence: the influence of LCPUFA on neural development, aging, and neurodegeneration. Prog Lipid Res 53, 1–17. doi:10.1016/j.plipres.2013.10.002.

Joie, R.L., Visani, A.V., Baker, S.L., Brown, J.A., Bourakova, V., Cha, J., Chaudhary, K., Edwards, L., Iaccarino, L., Janabi, M., Lesman-Segev, O.H., Miller, Z.A., Perry, D.C., O'Neil, J.P., Pham, J., Rojas, J.C., Rosen, H.J., Seeley, W.W., Tsai, R.M., Miller, B.L., Jagust, W.J., Rabinovici, G.D., 2020. Prospective longitudinal atrophy in Alzheimer's disease correlates with the intensity and topography of baseline tau-PET. Sci Transl Med 12. doi:10.1126/scitranslmed.aau5732.

Khalil, M., Pirpamer, L., Hofer, E., Voortman, M.M., Barro, C., Leppert, D., Benkert, P., Ropele, S., Enzinger, C., Fazekas, F., Schmidt, R., Kuhle, J., 2020. Serum neurofilament light levels in normal aging and their association with morphologic brain changes. Nat Commun 11, 812. doi:10.1038/s41467-020-14612-6.

Khalil, M., Teunissen, C.E., Otto, M., Piehl, F., Sormani, M.P., Gattringer, T., Barro, C., Kappos, L., Comabella, M., Fazekas, F., Petzold, A., Blennow, K., Zetterberg, H., Kuhle, J., 2018. Neurofilaments as biomarkers in neurological disorders. Nat Rev Neurol 14, 577–589. doi:10.1038/s41582-018-0058-z.

Lépinoux-Chambaud, C., Eyer, J., 2013. Review on intermediate filaments of the nervous system and their pathological alterations. Histochem. Cell Biol. 140, 13–22. doi:10.1007/s00418-013-1101-1.

Markello, R.D., Arnatkeviciute, A., Poline, J.-B., Fulcher, B.D., Fornito, A., Misic, B., 2021. Standardizing workflows in imaging transcriptomics with the abagen toolbox. eLife 10, e72129. doi: 10.7554/eLife.72129

Márquez, F., Yassa, M.A., 2019. Neuroimaging Biomarkers for Alzheimer's Disease. Mol Neurodegener 14, 21. doi:10.1186/s13024-019-0325-5.

Mattsson, N., Andreasson, U., Zetterberg, H., Blennow, K., 2017. Association of plasma neurofilament light with neurodegeneration in patients with alzheimer disease. JAMA Neurol 74, 557–566. doi:10.1001/jamaneurol.2016.6117.

Mattsson, N., Cullen, N.C., Andreasson, U., Zetterberg, H., Blennow, K., 2019. Association between longitudinal plasma neurofilament light and neurodegeneration in patients with alzheimer disease. JAMA Neurol 76, 791–799. doi:10.1001/jamaneurol.2019.0765.

Mielke, M.M., Syrjanen, J.A., Blennow, K., Zetterberg, H., Skoog, I., Vemuri, P., Machulda, M.M., Graff-Radford, J., Knopman, D.S., Jack, C.R., Petersen, R.C., Kern, S., 2019. Comparison of variables associated with cerebrospinal fluid neurofilament, total-tau, and neurogranin. Alzheimers Dement 15, 1437–1447. doi:10.1016/j.jalz.2019.07.009.

Morris, J.C., 1993. The Clinical Dementia Rating (CDR): current version and scoring rules. Neurology 43, 2412–2414.

Moullé, V.S.F., Cansell, C., Luquet, S., Cruciani-Guglielmacci, C., 2012. The multiple roles of fatty acid handling proteins in brain. Front. Physio. 3. doi:10.3389/fphys.2012.00385.

Mueller, S.G., Weiner, M.W., Thal, L.J., Petersen, R.C., Jack, C., Jagust, W., Trojanowski, J.Q., Toga, A.W., Beckett, L., 2005. The Alzheimer's disease neuroimaging initiative. Neuroimaging Clin. N. Am. 15, 869–877. doi:10.1016/j.nic.2005.09.008, xi–xiidoi:.

Nyberg, L., Lundquist, A., Nordin Adolfsson, A., Andersson, M., Zetterberg, H., Blennow, K., Adolfsson, R., 2020. Elevated plasma neurofilament light in aging reflects brain white-matter alterations but does not predict cognitive decline or Alzheimer's disease. Alzheimer's & Dementia: Diagnosis. Assessment & Disease Monitoring 12, e12050. doi:10.1002/dad2.12050.

Obrocki, P., Khatun, A., Ness, D., Senkevich, K., Hanrieder, J., Capraro, F., Mattsson, N., Andreasson, U., Portelius, E., Ashton, N.J., Blennow, K., Schöll, M., Paterson, R.W., Schott, J.M., Zetterberg, H., 2020. Perspectives in fluid biomarkers in neurodegeneration from the 2019 biomarkers in neurodegenerative diseases course-a joint PhD student course at University College London and University of Gothenburg. Alzheimers Res Ther 12, 20. doi:10.1186/s13195-020-00586-6.

O'Bryant, S.E., Xiao, G., Edwards, M., Devous, M., Gupta, V.B., Martins, R., Zhang, F., Barber, R., 2013. Biomarkers of Alzheimer's disease among Mexican Americans. J Alzheimers Dis 34, 841–849. doi:10.3233/JAD-122074.

Olsson, B., Alberg, L., Cullen, N.C., Michael, E., Wahlgren, L., Kroksmark, A.-K., Rostasy, K., Blennow, K., Zetterberg, H., Tulinius, M., 2019. NFL is a marker of treatment response in children with SMA treated with nusinersen. J Neurol 266, 2129–2136. doi:10.1007/s00415-019-09389-8.

Olsson, B., Hertze, J., Ohlsson, M., Nägga, K., Höglund, K., Basun, H., Annas, P., Lannfelt, L., Andreasen, N., Minthon, L., Zetterberg, H., Blennow, K., Hansson, O., 2013. Cerebrospinal fluid levels of heart fatty acid binding protein are elevated prodromally in Alzheimer's disease and vascular dementia. J. Alzheimers Dis. 34, 673–679. doi:10.3233/JAD-121384.

Pak, J.H., Huang, F.L., Li, J., Balschun, D., Reymann, K.G., Chiang, C., Westphal, H., Huang, K.-P., 2000. Involvement of neurogranin in the modulation of calcium/calmodulin-dependent protein kinase II, synaptic plasticity, and spatial learning: A study with knockout mice. Proc Natl Acad Sci 97, 11232–11237. doi:10.1073/pnas.210184697.

Pégorier, J.-P., May, C.L., Girard, J., 2004. Control of gene expression by fatty acids. J Nutr 134, 2444S–2449S. doi:10.1093/jn/134.9.2444S.

Pelsers, M.M.A.L., Hanhoff, T., Van Der Voort, D., Arts, B., Peters, M., Ponds, R., Honig, A., Rudzinski, W., Spener, F., De Kruijk, J.R., Twijnstra, A., Hermens, W.T., Menheere, P.P.C.A., Glatz, J.F.C., 2004. Brain- and heart-type fatty acid-binding proteins in the brain: Tissue distribution and clinical utility. Clin Chem 50, 1568–1575. doi:10.1373/clinchem.2003.030361.

Pereira, J.B., Janelidze, S., Ossenkoppele, R., Kvartsberg, H., Brinkmalm, A., Mattsson-Carlgren, N., Stomrud, E., Smith, R., Zetterberg, H., Blennow, K., Hansson, O.,

2021. Untangling the association of amyloid-β and tau with synaptic and axonal loss in Alzheimer's disease. Brain 144, 310–324. doi:10.1093/brain/awaa395.
Pereira, J.B., Westman, E., Hansson, O., 2017. Association between cerebrospinal fluid and plasma neurodegeneration biomarkers with brain atrophy in Alzheimer's disease. Neurobiol Aging 58, 14–29. doi:10.1016/j.neurobiolaging.2017.06.002.
Peters, A., Sethares, C., 2002. The effects of age on the cells in layer 1 of primate cerebral cortex. Cereb. Cortex 12, 27–36.
Petzold, A., 2005. Neurofilament phosphoforms: Surrogate markers for axonal injury, degeneration and loss. Journal of the Neurological Sciences, Preserve the Neuron. 233, 183–198. doi:10.1016/j.jns.2005.03.015.
Portelius, E., Zetterberg, H., Skillbäck, T., Törnqvist, U., Andreasson, U., Trojanowski, J.Q., Weiner, M.W., Shaw, L.M., Mattsson, N., Blennow, K., 2015. Cerebrospinal fluid neurogranin: relation to cognition and neurodegeneration in Alzheimer's disease. Brain 138, 3373–3385. doi:10.1093/brain/awv267.
Reuter, M., Schmansky, N.J., Rosas, H.D., Fischl, B., 2012. Within-subject template estimation for unbiased longitudinal image analysis. Neuroimage 61, 1402–1418. doi:10.1016/j.neuroimage.2012.02.084.
Rohrer, J.D., Woollacott, I.O.C., Dick, K.M., Brotherhood, E., Gordon, E., Fellows, A., Toombs, J., Druyeh, R., Cardoso, M.J., Ourselin, S., Nicholas, J.M., Norgren, N., Mead, S., Andreasson, U., Blennow, K., Schott, J.M., Fox, N.C., Warren, J.D., Zetterberg, H., 2016. Serum neurofilament light chain protein is a measure of disease intensity in frontotemporal dementia. Neurology 87, 1329–1336. doi:10.1212/WNL.0000000000003154.
Romero-Garcia, R., Whitaker, K.J., Váša, F., Seidlitz, J., Shinn, M., Fonagy, P., Dolan, R.J., Jones, P.B., Goodyer, I.M., Bullmore, E.T., Vértes, P.E., 2018. Structural covariance networks are coupled to expression of genes enriched in supragranular layers of the human cortex. Neuroimage 171, 256–267. doi:10.1016/j.neuroimage.2017.12.060.
Shaw, L.M., Vanderstichele, H., Knapik-Czajka, M., Clark, C.M., Aisen, P.S., Petersen, R.C., Blennow, K., Soares, H., Simon, A., Lewczuk, P., Dean, R., Siemers, E., Potter, W., Lee, V.M.-Y., Trojanowski, J.Q., 2009. Cerebrospinal fluid biomarker signature in alzheimer's disease neuroimaging initiative subjects. Ann Neurol 65, 403–413. doi:10.1002/ana.21610.
Shaw, L.M., Vanderstichele, H., Knapik-Czajka, M., Figurski, M., Coart, E., Blennow, K., Soares, H., Simon, A.J., Lewczuk, P., Dean, R.A., Siemers, E., Potter, W., Lee, V.M.-Y., Trojanowski, J.Q., 2011. Qualification of the analytical and clinical performance of CSF biomarker analyses in ADNI. Acta Neuropathol 121, 597–609. doi:10.1007/s00401-011-0808-0.
Sørensen, Ø., Walhovd, K.B., Fjell, A.M., 2021. A recipe for accurate estimation of lifespan brain trajectories, distinguishing longitudinal and cohort effects. Neuroimage 226, 117596. doi:10.1016/j.neuroimage.2020.117596.
Subramanian, A., Tamayo, P., Mootha, V.K., Mukherjee, S., Ebert, B.L., Gillette, M.A., Paulovich, A., Pomeroy, S.L., Golub, T.R., Lander, E.S., Mesirov, J.P., 2005. Gene set enrichment analysis: a knowledge-based approach for interpreting genome-wide expression profiles. Proc Natl Acad Sci 102, 15545–15550. doi:10.1073/pnas.0506580102.
Tibshirani, R., 1996. Regression shrinkage and selection via the lasso. Journal of the Royal Statistical Society: Series B (Methodological) 58, 267–288. doi:10.1111/j.2517-6161.1996.tb02080.x.
Tucker-Drob, E.M., 2019. Cognitive aging and dementia: a life-span perspective. Annual Review of Developmental Psychology 1, 177–196. doi:10.1146/annurev-devpsych-121318-085204.
Vågberg, M., Norgren, N., Dring, A., Lindqvist, T., Birgander, R., Zetterberg, H., Svenningsson, A., 2015. Levels and age dependency of neurofilament light and glial fibrillary acidic protein in healthy individuals and their relation to the brain parenchymal fraction. PLoS One 10, e0135886. doi:10.1371/journal.pone.0135886.
Vidal-Pineiro, D., Wang, Y., Krogsrud, S.K., Amlien, I.K., Baaré, W.F., Bartres-Faz, D., Bertram, L., Brandmaier, A.M., Drevon, C.A., Düzel, S., Ebmeier, K., Henson, R.N., Junqué, C., Kievit, R.A., Kühn, S., Leonardsen, E., Lindenberger, U., Madsen, K.S., Magnussen, F., Mowinckel, A.M., Nyberg, L., Roe, J.M., Segura, B., Smith, S.M., Sørensen, Ø., Suri, S., Westerhausen, R., Zalesky, A., Zsoldos, E., Walhovd, K.B., Fjell, A., 2021. Individual variations in 'brain age' relate to early-life factors more than to longitudinal brain change. eLife 10, e69995. doi:10.7554/eLife.69995.
Wyss-Coray, T., 2016. Ageing, neurodegeneration and brain rejuvenation. Nature 539, 180–186. doi:10.1038/nature20411.
Zetterberg, H., Blennow, K., 2018. From cerebrospinal fluid to blood: the third wave of fluid biomarkers for alzheimer's disease. J. Alzheimers Dis. 64, S271–S279. doi:10.3233/JAD-179926.
Zetterberg, H., Skillbäck, T., Mattsson, N., Trojanowski, J.Q., Portelius, E., Shaw, L.M., Weiner, M.W., Blennow, K., 2016. Association of cerebrospinal fluid neurofilament light concentration with alzheimer disease progression. JAMA Neurol 73, 60–67. doi:10.1001/jamaneurol.2015.3037.
Zuo, X.-N., Xu, T., Milham, M.P., 2019. Harnessing reliability for neuroscience research. Nat Hum Behav 3, 768–771. doi:10.1038/s41562-019-0655-x.